

Incremental displacement estimation of structures using paired structured light

Haemin Jeon¹, Jae-Uk Shin² and Hyun Myung^{*,1,2}

¹Department of Civil and Environmental Engineering, KAIST, Daejeon 305-701, Korea

²Robotics Program, KAIST, Daejeon 305-701, Korea

(Received June 13, 2011, Revised February 3, 2012, Accepted February 27, 2012)

Abstract. As civil structures are exposed to various external loads, it is essential to assess the structural condition, especially the structural displacement, in every moment. Therefore, a visually servoed paired structured light system was proposed in the previous study. The proposed system is composed of two screens facing with each other, each with a camera, a screen, and one or two lasers controlled by a 2-DOF manipulator. The 6-DOF displacement can be calculated from the positions of three projected laser beams and the rotation angles of the manipulators. In the estimation process, one of well-known iterative methods such as Newton-Raphson or extended Kalman filter (EKF) was used for each measurement. Although the proposed system with the aforementioned algorithms estimates the displacement with high accuracy, it takes relatively long computation time. Therefore, an incremental displacement estimation (IDE) algorithm which updates the previously estimated displacement based on the difference between the previous and the current observed data is newly proposed. To validate the performance of the proposed algorithm, simulations and experiments are performed. The results show that the proposed algorithm significantly reduces the computation time with the same level of accuracy compared to the EKF with multiple iterations.

Keywords: SHM (structural health monitoring); displacement; IDE (incremental displacement estimation); vision; laser

1. Introduction

As structural health monitoring (SHM) has gained great attention for several decades, various monitoring systems or sensors have been developed (Balageas *et al.* 2006). Especially, the structural displacement monitoring is considered as one of the important safety indicators to assess the structural condition (Ji and Chang 2008, Ni *et al.* 2011). To measure the structural displacement, conventional sensors such as accelerometers, GPS, and LVDTs have been widely used. However, these sensors have one of following problems; a) it indirectly measures the displacement, b) the cost is relatively high, or c) it is hard to install or maintain. For example, the accelerometer which is one of the widely used sensors measures the displacement by integrating the acceleration signal twice. Due to the signal drift, however, the integrated displacement is neither stable nor accurate (Park *et al.* 2005). As another example, GPS estimates the displacement with high accuracy. Especially the best class RTK (Real Time Kinematic)-GPS can measure the displacement with an accuracy of a few

*Corresponding author, Professor, E-mail: hmyung@kaist.ac.kr

millimeters, while the cost is relatively high (more than 20,000 USD for static RTK-GPS and 150,000 USD for dynamic RTK-GPS) (Psimoulis *et al.* 2008, Xu *et al.* 2009, Casciati and Fuggini 2011).

To solve the problems, various vision-based displacement monitoring systems have been researched as alternative solutions. Most of the vision-based displacement monitoring systems install the targets on the structure and a camera on a fixed point captures the movement of the targets from afar (Marecos *et al.* 1969, Leith *et al.* 1989, Stephen *et al.* 1993, Olaszek 1999, Wahbeh *et al.* 2003, Lee and Shinozuka 2006, Ni 2009, Park *et al.* 2010). Although the vision-based displacement monitoring system directly estimates the displacement with the relatively low cost, the displacement can be estimated only if the line of sight is assured. In other words, most of the vision-based systems are highly affected by the external changes such as weather or illumination since the distance between the camera and the target is relatively long.

Therefore, Myung *et al.* (2011) suggested a paired structured light (SL) system to directly estimate the displacement while keeping the cost relatively cheap and making it robust to the external environmental changes. The proposed system is composed of two screens facing with each other, each with a camera, a screen, and one or two lasers. In this system, the laser on each side projects its parallel beam to the screen on the opposite side and 6-DOF displacement between two sides can be calculated from the positions of the three projected laser beams. Though the proposed system can be used to successfully estimate the translational and rotational displacement each in 3-DOF, the observable range is limited by the limited screen size. To mitigate this problem, Jeon *et al.* (2011) proposed a visually servoed paired structured light system (ViSP) which combines the visual servoing technique to the former paired SL system. The idea of the proposed system is to control the positions of the projected laser beams to be on the screen all the time. Since the manipulators force the projected laser beams to be inside the screen boundary, the proposed system can estimate the displacement regardless of its magnitude. Furthermore, the proposed system is significantly economical compared to the cost of GPS since the total cost of the proposed system including PCs, lasers, cameras, motors, and bluetooths is roughly 2,000 USD.

The kinematic equation of this system represents the relationship between the displacement and the observed positions of projected laser beams which are controlled by the manipulator. To solve the kinematics, the conventional iterative method such as Newton-Raphson or extended Kalman filter (EKF) was used assuming the displacement is stationary in a short time interval. However, these iterative methods take relatively long computation time to converge and the estimation of displacement cannot be done in one cycle at high frequencies of motion. To cope with this problem, novel incremental displacement estimation (IDE) algorithm which updates the previously estimated displacement with the difference of the previous and the current projected laser beam positions is introduced. Since the proposed algorithm directly calculates the updated displacement just in one cycle, it is more suitable for estimating the dynamic displacement in comparison with the conventional iterative algorithms. The remainder of this paper is organized as follows. In Section 2, the configuration of the ViSP is described. In Section 3, the kinematics of the system and the incremental displacement estimation algorithm are presented. In Section 4, simulations and experiments were conducted to validate the performance of the proposed algorithm. Conclusions are discussed in Section 5.

2. Visually servoed paired structured light system

To estimate the 6-DOF displacement of structures, the ViSP was proposed (Jeon *et al.* 2011). The

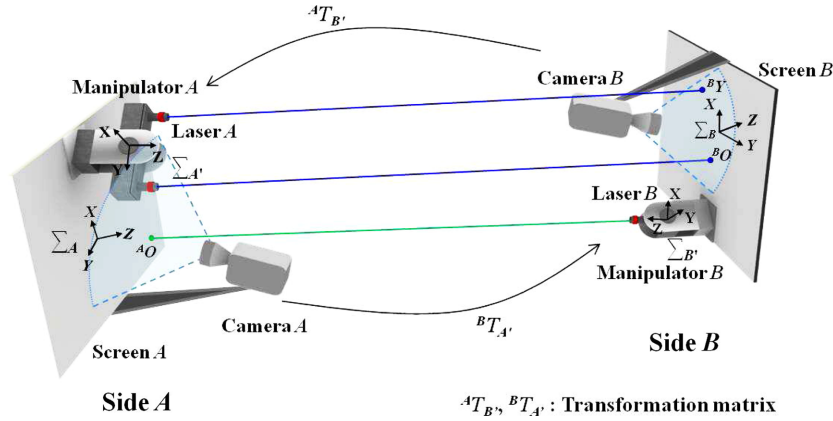


Fig. 1 A schematic diagram of the visually servoed paired structured light system (Jeon *et al.* 2011)

conventional SL is the process of projecting simple pattern of beam to a screen and a depth and surface information are calculated from the captured images (Siegwart and Nourbakhsh 2004). Similar to the conventional SL system, the proposed system projects laser beams and the translational and the rotational displacement between two sides are calculated from the positions of the projected laser beams and the rotation angles of the manipulators. As shown in Fig. 1, one module of the proposed system is composed of two screens facing with each other, each with a camera, a screen, and one or two lasers controlled by the 2-DOF manipulator. As shown in the figure, each laser projects its parallel beam to the opposite screen and the camera near the screen captures the image of the screen. The 2-DOF manipulator controls the positions of the projected laser beams to be on the 2D screen all the time. Due to the relatively short distance from the screen to the camera, typically less than 20 cm, the proposed system is less likely to be affected by the external conditions such as weather or illumination changes. In the figure, Σ_A and $\Sigma_{A'}$ represent respectively the coordinate frames of the screen and the laser on side A. Similarly, Σ_B and $\Sigma_{B'}$ represent respectively the screen coordinate frame and the laser coordinate frame on side B.

The entire process of the proposed system is shown in Fig. 2. At first, the camera on each side captures the image and a lens distortion is corrected. From the undistorted image, the boundary of the screen is extracted. Since the screen size is known, the positions of the projected laser beams

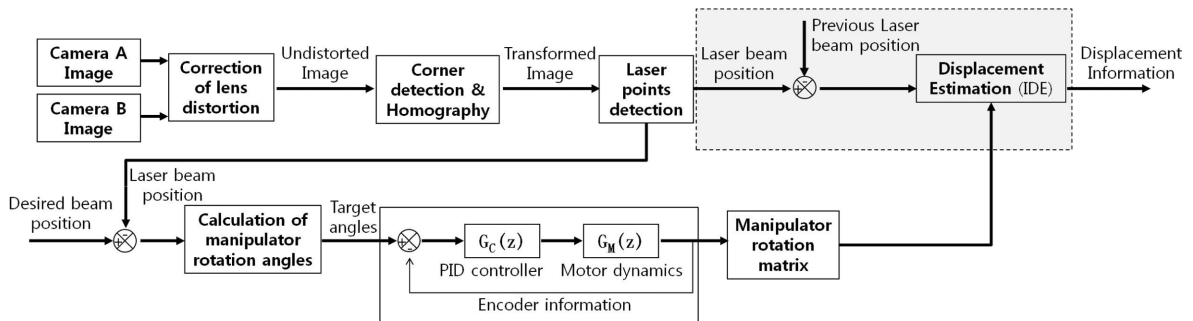


Fig. 2 A block diagram of the displacement estimation process with the visually servoed 2-DOF manipulator. IDE: Incremental Displacement Estimation algorithm

inside the screen boundary can be calculated. Then, the rotation angles of the manipulators are calculated so as to minimize the difference between the desired and the current laser beam positions. In this paper, the desired laser beam position is set to be the center of the screen. The calculated rotation angles are inputted to the PID controller and the encoder information of the motors forms the manipulator rotation matrix. From the manipulator rotation matrices on both sides and the positions of the three projected laser beams, the 6-DOF displacement can be calculated by the newly proposed incremental displacement estimation algorithm since each laser position provides two data; x and y positions.

3. Incremental displacement estimation algorithm

3.1 Kinematics of the visually servoed paired structured light system

The kinematics defines the geometric relationship between the observed data $m = [{}^A O, {}^B O, {}^B Y]^T$ and the actual displacement $p = [x, y, z, \theta, \phi, \psi]^T$. Here ${}^A O$ is the projected laser beam on screen A , ${}^B O$ and ${}^B Y$ are the projected laser beams on screen B . To derive the kinematics, the transformation matrices ${}^A T_B$ and ${}^B T_A$ are used. The ${}^A T_B$ is a transformation matrix that transforms the Σ_B to the Σ_A consists of the product of translation matrix $T(x, y, z)$ along the X , Y , and Z axes and the rotation matrices $R_x(\theta)$, $R_y(\phi)$, and $R_z(\psi)$ about the X , Y , and Z axes, respectively, as follows

$${}^A T_B(x, y, z, \theta, \phi, \psi) = T(x, y, z)R_x(\theta)R_y(\phi)R_z(\psi)$$

$$= \begin{bmatrix} c_\phi c_\psi & -c_\phi s_\psi & s_\phi & x \\ s_\theta s_\phi c_\psi + c_\theta s_\psi & -s_\theta s_\phi s_\psi + c_\theta s_\psi & -s_\theta c_\phi & y \\ -c_\theta s_\phi c_\psi + s_\theta s_\psi & c_\theta s_\phi s_\psi + s_\theta s_\psi & c_\theta c_\phi & z \\ 0 & 0 & 0 & 1 \end{bmatrix} \quad (1)$$

where θ , ϕ , and ψ are the rotation angles about X , Y , and Z axes, s_θ and c_θ denote $\sin\theta$ and $\cos\theta$, respectively. Since the observed data m is controlled by the manipulator which rotates along X and Z axes, not only the transformation matrix ${}^A T_B$ or ${}^B T_A$ but also the manipulator rotation matrix ${}^A T_{A'}$ or ${}^B T_{B'}$ should be considered where ${}^A T_{A'}$ and ${}^B T_{B'}$ represent the transformation matrices that transform $\Sigma_{A'}$ to Σ_A and $\Sigma_{B'}$ to Σ_B , respectively. In other words, the transformation matrix (${}^A T_B$) and manipulator rotation matrix on side B , ${}^B T_{B'} = R_x(-\theta_{Benc}) \cdot R_z(-\psi_{Benc})$, are used to calculate the position of the projected laser beam ${}^A O$ as follows

$${}^A O = {}^A T_B \cdot {}^B T_{B'} [0 \ 0 \ Z_{AB} \ 1]^T \quad (2)$$

where θ_{Benc} and ψ_{Benc} are rotated angles of the manipulator on side B about X and Z axes, respectively, and Z_{AB} is the distance in Z direction between Σ_A and Σ_B . Similar to ${}^A O$, ${}^B O$ and ${}^B Y$ can be obtained as follows

$${}^B O = {}^B T_A \cdot {}^A T_{A'} [0 \ -L \ Z_{AB} \ 1]^T \quad (3)$$

$${}^B Y = {}^B T_A \cdot {}^A T_{A'} [0 \ L \ Z_{AB} \ 1]^T \quad (4)$$

where L is the offset of the installed laser position from the center of a screen in Y direction. As z should be zero on the projected 2D screen, the z component of ${}^A O$, ${}^B O$, and ${}^B Y$ are set to zero. By putting three constraints (2)-(4) altogether, the kinematic equation M_{vs} containing 6-DOF displacement p can be derived as follows (Jeon *et al.* 2011)

$$M_{vs} = \begin{bmatrix} {}^A O_x & {}^A O_y & {}^B O_x & {}^B O_y & {}^B Y_x & {}^B Y_y \end{bmatrix}^T$$

$$= \begin{bmatrix} -(xc_{\theta_B}c_{\psi_B} + Z_{AB}(c_{\theta_B}c_{\psi_B}s_{\phi} + s_{\theta_B}s_{\psi_B})) + xs_{\theta_B}s_{\psi_B}s_{\phi} + ys_{\psi_B}c_{\phi} / (c_{\theta_B}c_{\psi}) \\ (xs_{\theta_B}c_{\psi_B} + Z_{AB}(c_{\theta_B}s_{\psi_B}s_{\phi} - s_{\theta_B}c_{\psi_B})) - xs_{\theta_B}c_{\psi_B}s_{\phi} + yc_{\psi_B}c_{\phi} / (c_{\theta_B}c_{\psi}) \\ (2c_{\phi}c_{\theta_A}s_{\theta_A}s_{\phi}(c_{\theta_A} + c_{\psi_A})L - (c_{\theta_A}c_{\psi_A} - s_{\theta_A}s_{\psi_A}s_{\phi})x - s_{\psi_A}c_{\phi}(y + L)) / (c_{\theta_A}c_{\phi}) \\ -(2c_{\theta_A}c_{\phi}(s_{\theta_A}s_{\phi}s_{\psi_A} - c_{\theta_A}c_{\psi_A})L - (c_{\theta_A}s_{\psi_A} + s_{\theta_A}c_{\psi_A}s_{\phi})x + c_{\psi_A}c_{\phi}(L + y)) / (c_{\theta_A}c_{\phi}) \\ (-c_{\theta_A}c_{\psi_A}x + s_{\psi_A}c_{\phi}L + s_{\theta_A}s_{\psi_A}s_{\phi}x - s_{\psi_A}c_{\phi}y) / (c_{\theta_A}c_{\phi}) \\ (c_{\theta_A}s_{\psi_A}x + c_{\psi_A}c_{\phi}L + s_{\theta_A}c_{\psi_A}s_{\phi}x - c_{\psi_A}c_{\phi}y) / (c_{\theta_A}c_{\phi}) \end{bmatrix} \quad (5)$$

where ${}^A O_x$ and ${}^A O_y$ denote the x and y component of ${}^A O$, respectively. $\theta_{\bar{B}} = \theta_{AB} - \theta_B$ where θ_{AB} is the rotation angle from Σ_A to Σ_B about X axis, and θ_B is the rotation angle between Σ_B and $\Sigma_{B'}$ about X axis. Similar to $\theta_{\bar{B}}$, $\psi_{\bar{B}} = \psi_{AB} - \psi_B$, $\theta_{\bar{A}} = \theta_{AB} - \theta_A$ and $\psi_{\bar{A}} = \psi_{AB} - \psi_A$.

3.2 Incremental displacement estimation algorithm

In the previous studies (Myung *et al.* 2011, Jeon *et al.* 2011), from the nonlinear kinematic equation M_{vs} , the displacement p was calculated by using the iterative methods such as Newton-Raphson or EKF for each measurement. In other words, the iterative methods had been used based on the assumption that the displacement is stationary in a short time interval for static and dynamic cases. In these iterative methods, however, the estimation of displacement cannot be done in one cycle at high frequency of motion as the computation time is relatively long. Therefore, the incremental displacement estimation (IDE) algorithm is newly proposed in this section. In this algorithm, the 6-DOF displacement is calculated by updating the previously estimated displacement based on the difference between the current position of the projected laser beam and the previous one.

Before going further, let us explain the difference of the sampling time notation. As shown in Fig. 3, the sampling time of the measurement data is T_{s1} and the iterative computation is performed with the sampling time of T_{s2} between each sampling time of T_{s1} . Let us denote the time steps as t and k for sampling times T_{s1} and T_{s2} . The estimation of the displacement \hat{p} by using Newton-Raphson method can be represented as follows (Myung *et al.* 2011, Jeon *et al.* 2011)

$$\hat{m}(k) = M_{vs}(\hat{p}(k))$$

$$\hat{p}(k+1) = \hat{p}(k) + J_p^+(m(k) - \hat{m}(k)) \quad (6)$$

where $\hat{m}(k)$ is the estimated measurement by M_{vs} , $m(k)$ is the measured positions of the projected laser beams, $J_p = \partial M_{vs} / \partial p$ is the Jacobian of the kinematic equation, and J_p^+ is the pseudo-inverse of the Jacobian.

In case there exist uncertainties in the measurement, the EKF algorithm (Welch and Bishop 2006) can be applied to estimate the displacement \hat{p} . In the prediction step of the EKF, prediction of the

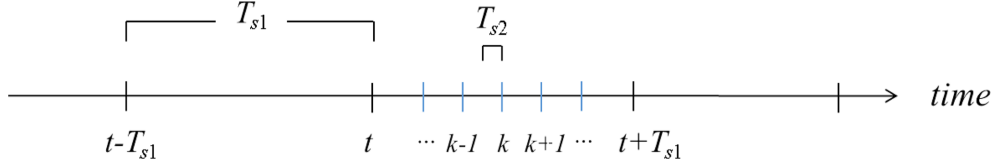


Fig. 3 The sampling time of the measurement data is T_{s1} . The iterative computation is performed with the sampling time T_{s2} between each sampling time of T_{s1}

displacement (\hat{p}) and measurement (\hat{m}) can be obtained as follows

$$\begin{aligned}\hat{p}(k+1|k) &= \hat{p}(k|k) \\ \hat{m}(k+1|k) &= M_{vs}(\hat{p}(k+1|k)) \\ P(k+1|k) &= P(k|k) + Q\end{aligned}\quad (7)$$

where P is the error covariance matrix of the displacement, Q is the covariance matrix of the system noise, and M_{vs} is the kinematic equation obtained from Eq. (5), $(k+1|k)$ means *a priori* estimate and $(k+1|k+1)$ means *a posteriori* estimate where k is the iteration step.

In the observation step of the EKF, the following equation is applied

$$\begin{aligned}\nu(k+1) &= m(k+1) - \hat{m}(k+1|k) \\ S(k+1) &= J_p P(k+1|k) J_p^T + R\end{aligned}\quad (8)$$

where R is the covariance matrix of the measurement noise.

Finally, the EKF update step can be applied to obtain *a posteriori* result as follows

$$\begin{aligned}K(k+1) &= P(k+1|k) J_p^T S^{-1}(k+1) \\ \hat{p}(k+1|k+1) &= \hat{p}(k+1|k) + K(k+1) \nu(k+1) \\ P(k+1|k+1) &= P(k+1|k) - K(k+1) S(k+1) K^T(k+1)\end{aligned}\quad (9)$$

By doing so, the displacement \hat{p} and the displacement error covariance P can be estimated as well.

Similar to the EKF, the proposed algorithm is composed of prediction, observation, and update steps. In the prediction step of the proposed algorithm, \hat{p} is calculated by updating the previously estimated displacement based on the difference between the previous and the current positions of the projected laser beams. The prediction of the displacement (\hat{p}), measurement (\hat{m}), and displacement error covariance matrix (P) can be obtained as follows:

$$\begin{aligned}\hat{p}(t+1|t) &= \hat{p}(t|t) + J_p^+(t) \cdot \Delta m(t+1|t) \\ \hat{m}(t+1|t) &= M_{vs}(\hat{p}(t+1|t)) \\ P(t+1|t) &= P(t) + Q\end{aligned}\quad (10)$$

where $\Delta m(t+1|t)$ is the difference between the current and the previous projected laser beam positions

calculated by $\Delta m(t+1|t) = m(t+1) - \tilde{m}(t)$ where $\tilde{m}(t)$ are positions of the projected laser beams compensated by the current rotation angles of the manipulators. Compared to the prediction step of the EKF (Eq. (7)), the proposed algorithm predicts the displacement, $\hat{p}(t+1|t)$, by adding the difference of the displacement to the previously estimated displacement. The difference of the displacement can be calculated by multiplying $J_p^+(t)$ with $\Delta m(t+1|t)$.

After the prediction step, the observation and update steps are performed so as to minimize the error of the estimated and the actual positions of the projected laser beams. The observation step of the proposed algorithm can be obtained in a similar way as follows

$$\begin{aligned} v(t+1) &= m(t+1) - \hat{m}(t+1|t) \\ S(t+1) &= J_p(t+1) \cdot P(t+1|t) \cdot J_p^T(t+1|t) + R \end{aligned} \quad (11)$$

In the update step of the proposed algorithm, the following equation is applied

$$\begin{aligned} K(t+1) &= P(t+1|t) J_p^T(t+1) S^{-1}(t+1) \\ \hat{p}(t+1|t+1) &= \hat{p}(t+1|t) + K(t+1) v(t+1) \\ P(t+1|t+1) &= P(t+1) - K(t+1) S(t+1) K^T(t+1) \end{aligned} \quad (12)$$

It should be noted that the proposed algorithm is performed with the sampling time of T_{s1} , while the iterative algorithm is updated with the sampling time of T_{s2} . Since the proposed incremental algorithm uses the previous data, it cannot be applied at the first time step. Therefore, the iterative EKF method with multiple sub-iterations is used to find the initial displacement and the proposed algorithm is used afterwards.

4. Simulations and experiments

4.1 Simulation results

A simulation of estimating the dynamic displacement was conducted to validate the performance of the proposed algorithm. Three different algorithms; the proposed IDE, the EKF with 50 sub-iterations (EKF(50)), and the EKF with 1 sub-iteration that directly uses the previously estimated displacement and the displacement error covariance matrix (EKF(1)), have been applied to the displacement data from the second generation benchmark study proposed by Spencer *et al.* (1998). In the benchmark study, responses of the 20-story steel structure under the various seismic loads and various conditions such as existence of the controller or types of the structural evaluation model are described. In the following simulation, the calculated displacement of the roof, $(g(t))$, using the pre-earthquake evaluation model during the 1995 Kobe earthquake without a controller is used. In other words, the displacement of the simulation is set to as $p = (x_t, y_t, z_t, \theta_t, \phi_t, \psi_t) = (g(t), 0.01, 100, 0.05, 0.01, -0.01)$, where all units are meters and radians, with the random uniform measurement noise of $[-0.001, 0.001]$ m. Also, the covariance matrices of the system noise and the measurement noise are set to $Q = 1.0 \times 10^{-6}I$ and $R = 1.0 \times 10^{-6}I$, respectively. The estimation results using each algorithm were evaluated against the true values based on the root mean square error (RMSE) and the coefficient of cross-correlation (CORR). The RMSE and the CORR are defined by Eqs. (13) and (14), respectively.

Table 1 Root mean square errors (RMSE) and cross-correlation coefficients (CORR) of dynamic displacement estimation using three algorithms; the proposed incremental displacement estimation (IDE) algorithm, the EKF with 50 sub-iterations (EKF(50)), and the EKF with 1 sub-iteration (EKF(1)), respectively. The dimension of the computation time is msec/cycle

Algorithm	RMSE (mm)	RMSE (deg)	CORR	Avg. Computation Time
IDE	0.34	0.02	0.99	0.10
EKF(50)	0.56	0.15	0.99	4.25
EKF(1)	1.20	0.05	0.98	0.09

$$\text{RMSE} = \sqrt{\frac{\sum(x_{1,i} - x_{2,i})^2}{N}} \quad (13)$$

$$\text{CORR} = \frac{N\sum x_{1,i}x_{2,i} - (\sum x_{1,i})(\sum x_{2,i})}{\sqrt{N\sum x_{1,i}^2 - (\sum x_{1,i})^2} \sqrt{N\sum x_{2,i}^2 - (\sum x_{2,i})^2}} \quad (14)$$

where $x_{1,i}$, $x_{2,i}$, and N indicate the estimated displacement from each algorithm, ground truth, and the total number of data points, respectively; the subscript i indicates the i th data point.

The estimation results are illustrated in Table 1 and Fig. 4. As shown in the table, the computation time with the proposed algorithm and EKF(1) is significantly reduced by 98% compared to EKF(50). The proposed algorithm (IDE) shows better performance compared to the EKF(1). For example, it can be seen that the RMSEs for the proposed algorithm are 0.34 mm and 0.02° while the RMSEs for EKF(1) are 1.20 mm and 0.05°.

4.2 Experimental results

The experimental setup is illustrated in Fig. 5; one of two sides is laid on a shaking table and another on a fixed table. Two sides are set to be faced with each other and the lasers project their parallel beams to the opposite side. In this paper, the shaking table is used to make the artificial movement between two sides. To verify the performance of the system with the proposed algorithm, the estimated displacement is compared with the result from a laser displacement sensor (CD4-350, OPTEX FA Co., Ltd.). As shown in Fig. 6(a), each side is composed of a commercial camera, one or two lasers, a screen sized 150 mm×100 mm, and a 2-DOF manipulator. The calculated rotation angles of the manipulator are sent to the DSP (TI TMS320F2812) by a serial communication module as shown in Fig. 6(b) and the motors are controlled by the PID controller afterwards. The output encoder information from both motors is used to calculate the manipulator rotation matrix.

The displacement was estimated using three different algorithms, EKF(50), EKF(1), and IDE, and the laser displacement sensor. As in the simulations, the covariance matrices of the system noise and the measurement noise are set to $Q=1.0 \times 10^{-6}I$ and $R=1.0 \times 10^{-6}I$, respectively. The estimated translational displacements are shown in Figs. 7(a) and 8(a). As shown in Figs. 7(b) and 8(b), the estimation results from EKF(50), EKF(1), and IDE were compared with the laser displacement sensor which can be considered as a ground truth.

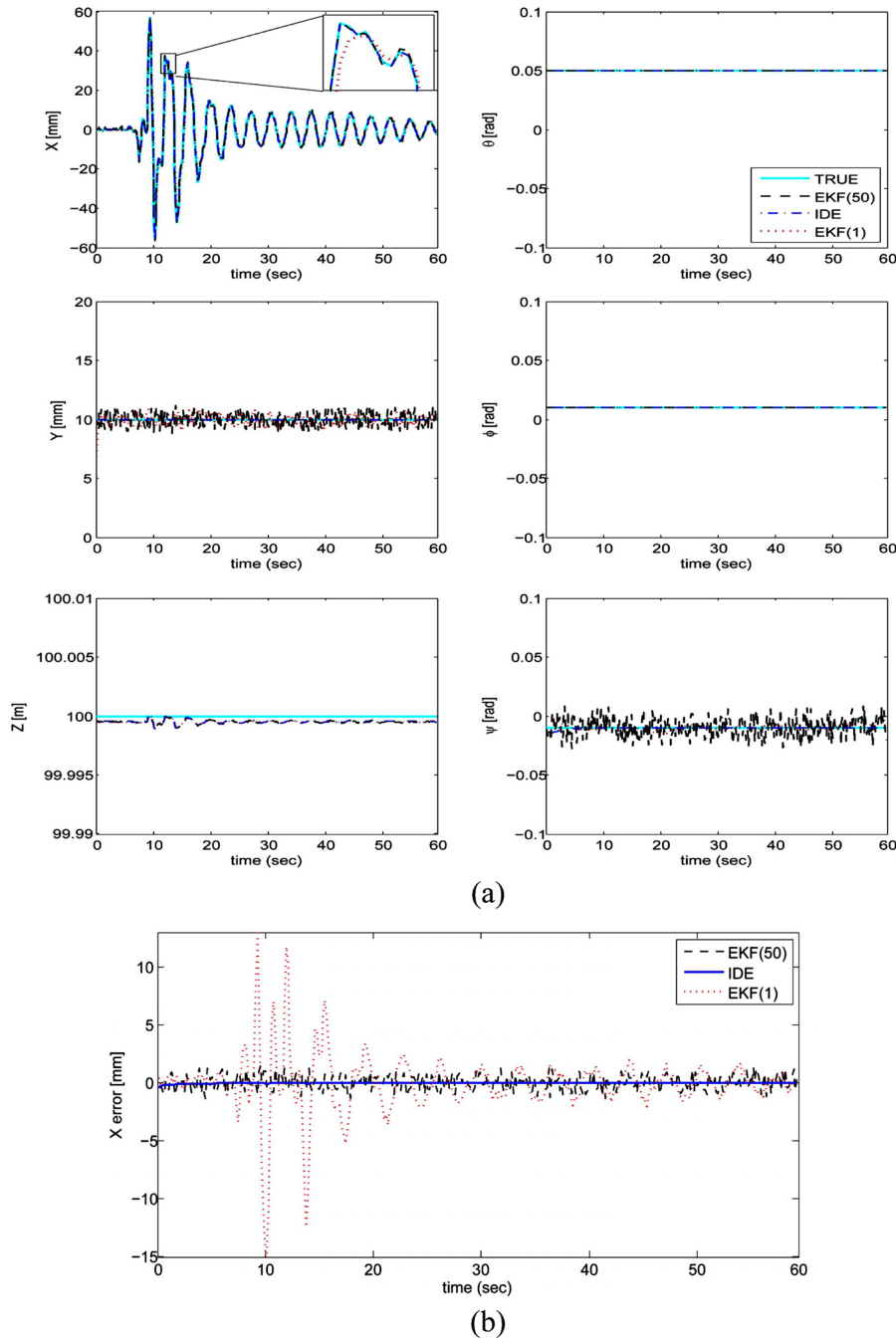


Fig. 4 Simulation results. (a) The estimated 6-DOF displacement from three algorithms. Dashed line: estimated displacement by using the EKF with the 50 sub-iterations (EKF(50)). Dashed dot line: estimated displacement by using the proposed incremental displacement estimation (IDE) algorithm. Dotted line: estimated displacement by using the EKF with 1 sub-iteration (EKF(1)). Solid line: the true value of $(x_t, y_t, z_t, \theta_t, \phi_t, \psi_t) = (g(t), 0.01, 100, 0.05, 0.01, -0.01)$, where all units are in meters and radians and (b) the error of the estimated X-axis translational displacement from each algorithm. Dashed line: error of the EKF(50). Solid line: error of the IDE. Dotted line: error of the EKF(1)

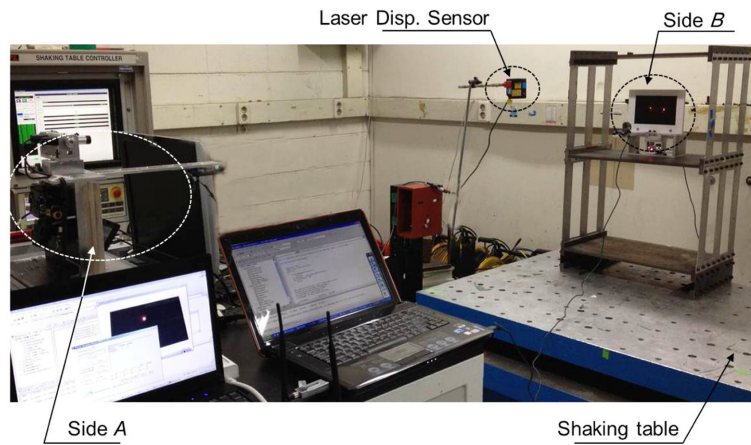


Fig. 5 The overall experimental setup. The distance between the two sides was set to 2 m

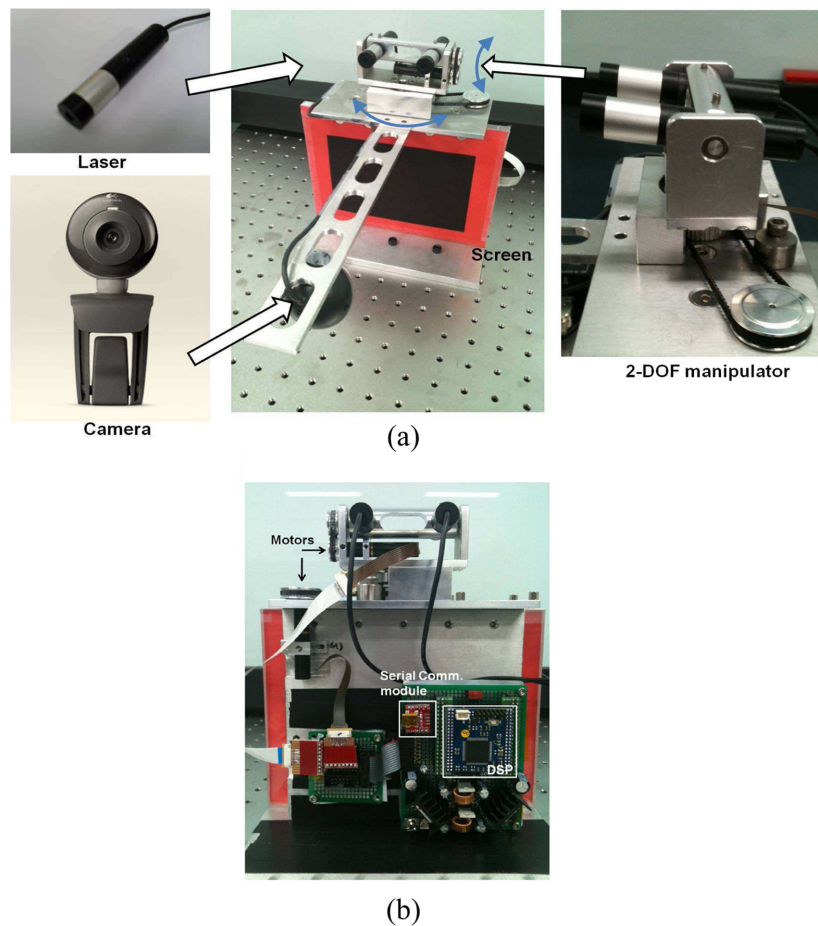


Fig. 6 The composition of one side of the module (Jeon *et al.* 2011). (a) A front view of one side of the module and (b) a rear view of one side of the module. The motors, the serial communication module, and DSP module are attached at the backside of the screen

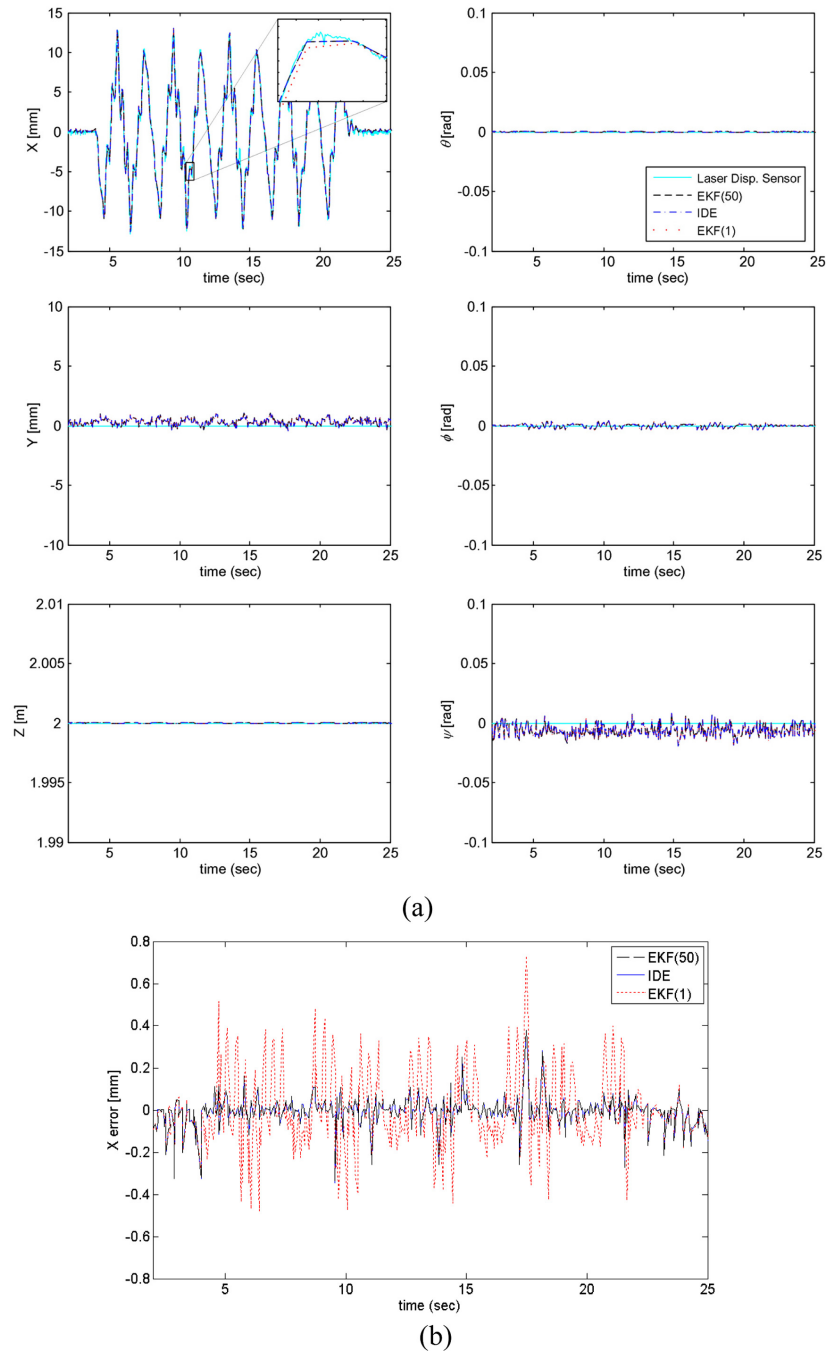


Fig. 7 Experimental results. (a) Estimated displacement of the dynamic translational displacement along X-axis. Solid line: result from the laser displacement sensor. Dashed line: estimated displacement by using the EKF with the 50 sub-iterations (EKF(50)). Dashed dot line: estimated displacement by using the proposed (IDE) algorithm. Dotted line: estimated displacement by using the EKF with 1 sub-iteration (EKF(1)) and (b) the error of the EKF(50) (Dashed line), IDE (Solid line), EKF(1) (Dotted line) in comparison with the laser displacement sensor, respectively

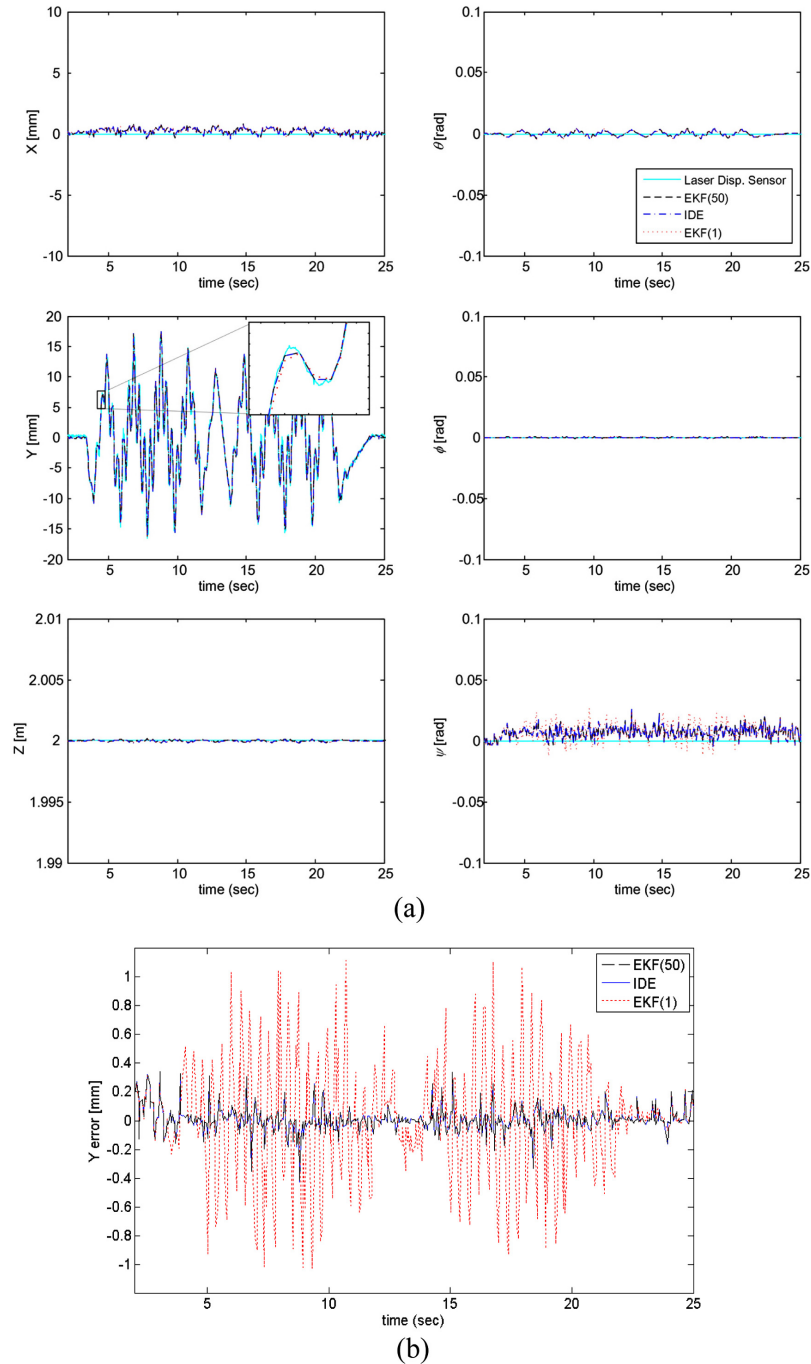


Fig. 8 Experimental results. (a) Estimated displacement of the dynamic translational displacement along Y -axis. Solid line: result from the laser displacement sensor. Dashed line: estimated displacement by using the EKF with the 50 sub-iterations (EKF(50)). Dashed dot line: estimated displacement by using the proposed (IDE) algorithm. Dotted line: estimated displacement by using the EKF with 1 sub-iteration (EKF(1)) and (b) the error of the EKF(50) (Dashed line), IDE (Solid line), EKF(1) (Dotted line) in comparison with the laser displacement sensor, respectively

Table 2 Root mean square error (RMSE) and cross-correlation coefficient (CORR) of translational displacement along X and Y axes, respectively. Compared to the EKF(50), the computation time of the proposed algorithm is significantly reduced by about 98%. The unit of the computation time is msec/cycle

Case	Algorithm	RMSE (mm)	RMSE (deg)	CORR	Avg. Computation Time
X axis	IDE	0.10	0.18	0.9999	0.09
	EKF(50)	0.10	0.18	0.9999	4.23
	EKF(1)	0.13	0.18	0.9995	0.08
Y axis	IDE	0.15	0.18	0.9999	0.09
	EKF(50)	0.15	0.18	0.9999	4.23
	EKF(1)	0.24	0.21	0.9984	0.09

The RMSE and CORR of the estimated displacement by using the three algorithms are presented in Table 2. It can be seen that the RMSEs of two cases with the proposed algorithm and EKF(50) are smaller than 0.15 mm and 0.18, and the CORRs are larger than 0.9999. On the other hand, the EKF(1) shows 0.24 mm and 0.21 as RMSEs and 0.9984 as CORR, respectively. These results show that the proposed system more accurately estimates the displacement than the EKF(1) with the same computation time.

5. Conclusions

In this paper, an incremental displacement estimation algorithm for the ViSP is proposed. In this algorithm, the displacement is predicted from the previously estimated displacement based on the difference between the previous and the current positions of the projected laser beams. After the prediction step, the observation and update steps are performed so as to minimize the error of the estimated and the actual positions of the projected laser points. By performing prediction, observation, and update steps of the proposed algorithm, the 6-DOF displacement can be estimated in real time.

To validate the performance of the proposed algorithm, the simulation and the experimental tests have been performed. The results show that the proposed algorithm can be used to estimate the displacement with the significantly reduced computation time with the same level of accuracy compared to the EKF(50). In comparison with the EKF(1), the proposed algorithm shows better performance with the same computation time. Because the proposed algorithm quickly estimates the displacement with high accuracy, the ViSP is more suitable solution for estimating the dynamic displacement. The advantage of the proposed algorithm is clearly seen under the rapidly oscillated displacement with the relatively large displacement as shown in the simulation result.

In the future, the multiple modules will be built and applicability of the proposed algorithm to large structures will be tested in a testing facility. Also the algorithm for minimization of the error propagation for multi-modules will be researched.

Acknowledgments

This work was supported by the National Research Foundation of Korea (NRF) grant funded by the Korea government (MEST) (grant number 2009-0075397).

References

- Balageas, D., Fritzen, C.P. and Guemes, A.(Eds.) (2006), *Structural Health Monitoring*, New Jersey, John Wiley& Sons.
- Casciati, F. and Fuggini, C. (2011), "Monitoring a steel building using GPS sensors", *Smart Struct.Syst.*, **7**(5), 349-363.
- Jeon, H., Bang, Y. and Myung, H. (2011), "A paired visual servoing system for 6-DOF displacement measurement of structures", *Smart Mater. Struct.*, **20**(4), 45019-45034.
- Ji, Y.F. and Chang, C.C. (2008), "Nontarget stereo vision technique for spatiotemporal response measurement of line-like structures", *J. Eng. Mech. - ASCE*, **134**(6), 466-474.
- Lee, J.J. and Shinozuka, M. (2006), "Real-time displacement measurement of a flexible bridge using digital image processing techniques", *Exp. Mech.*, **46**(1), 105-114.
- Leith, J.G., Thompson, A. and Sloan, T.D. (1989), "A novel dynamic deflection measurement system for large structure", *Proceedings of the 4th Int. Conf. on Civil and Structural Engineering Computing*, London.
- Marecos, J., Castanheira, M. and Trigo, J. (1969), "Field observation of Tagus river suspension bridge", *J. Struct. Div.- ASCE*, **95**(4), 555-583.
- Myung, H., Lee, S.M. and Lee, B.J. (2011), "Paired structured light for structural health monitoring robot system", *Struct. Health Monit.*, **10**(1), 49-64.
- Ni, Y.Q. (2009), "Fusion of vision-based displacement and acceleration using Kalman filter", *Proceedings of the 5th Int. Workshop on Advanced Smart Materials and Smart Structures Technology*, Boston.
- Ni, Y.Q., Wong, K.Y. and Xia, Y. (2011), "Health checks through land mark bridges to sky-high structures", *Adv. Struct. Eng.*, **14**(1), 103-119.
- Olaszek, P. (1999), "Investigation of the dynamic characteristic of bridge structures using a computer vision method", *Measurement*, **25**(3), 227-236.
- Park, J.W., Lee, J.J., Jung, H.J. and Myung, H. (2010), "Vision-based displacement measurement method for high-rise building structures using partitioning approach", *NDT & E Int.*, **43**(7), 642-647.
- Park, K.T., Kim, S.H., Park, H.S. and Lee, K.W. (2005), "The determination of bridge displacement using measured acceleration", *Eng. Struct.*, **27**(3), 371-378.
- Psimoulis, P., Pytharouli, S., Karambalis, D. and Stiros, S. (2008), "Potential of global positioning system (GPS) to measure frequencies of oscillations of engineering structures", *J. Sound Vib.*, **318**(3), 606-623.
- Sieglwart, R. and Nourbakhsh, I.R. (2004), *Introduction to Autonomous Mobile Robots*, MIT Press.
- Spencer, B.F., Jr., Christenson, R.E. and Dyke, S.J. (1998), "Next generation benchmark control problem for seismically excited buildings", *Proceedings of the 2nd Int. Conf. on Structural Control*, June 29-July 2.
- Stephen, G.A., Brownjohn, J.M.W. and Taylor, C.A. (1993), "Measurements of static and dynamic displacement from visual monitoring of the Humber bridge", *Eng. Struct.*, **15**(3), 197-208.
- Wahbeh, A.M., Caffrey, J.P. and Masri, S.F. (2003), "A vision-based approach for the direct measurement of displacements in vibrating systems", *Smart Mater. Struct.*, **12**(5), 785-794.
- Welch, G. and Bishop, G. (2006), *An introduction to the Kalman filter, TR95-041.*, Department of Computer Science, University of North Carolina, Chapel Hill.
- Xu, Y.L. and Chan, W.S. (2009), "Wind structural monitoring of long span cable-supported bridges with GPS", *Proceedings of the 7th Asia-Pacific Conference on Wind Engineering*, Taipei.